DENSIMETRIC EXCHANGE FLOW IN RECTANGULAR CHANNELS

IV - THE ARRESTED SALINE WEDGE

BY J. F. RIDDELL *

Introduction

The three previous papers of this series [1, 2, 3] concerned investigations of thermal and solution effect density currents formed by lock exchange flow. For this form of unsteady state densimetric flow, both finite and "infinite" lock lengths were considered. This fourth paper now describes a comprehensive range of experiments involving a case of steady state densimetric flow, the arrested saline wedge.

While lock exchange flow results from the rapid removal of a barrier separating two bodies of fluid of initial small density difference, the two bodies being at rest before the removal, figure 1 *a*, in the case of the arrested wedge one body of fluid is already moving as the other comes in contact with it. The most frequent occurrence of such a situation is likely where the more dense saline water of a sea or estuary meets the less dense fresh water of a flowing river or stream, figure 1 *b*. With suitable geographical and hydraulic conditions [4] the more dense sea water may penetrate upstream, underneath the less dense river flow while still retaining its distinct identity. The penetration proceeds until a balance is achieved between the capacity of the more dense water to supplant the river flow and the capacity of the river flow to dispel the intrusion. At this point of maximum penetration the underflow becomes arrested and the more dense intrusion extending downstream from the point of arrestment adopts a distinctive wedge shape.

The existence of the "salt wedge" or "highly stratified" type of estuary has been appreciated for some years and a number of researchers have undertaken laboratory and theoretical studies of the wedge itself and of the various problems associated with it. In the United States, systematic series of tests by Farmer [5] and by Farmer and Morgan [6] were followed by the extensive studies made by Keulegan [7, 8, 9] while Sanders, Maximom and Morgan [10] presented a theoretical analysis. Outside of the United States the work of Hinwood [12] and of Majewski [13] is of particular interest. (Schijf and Schönfeld [11] also

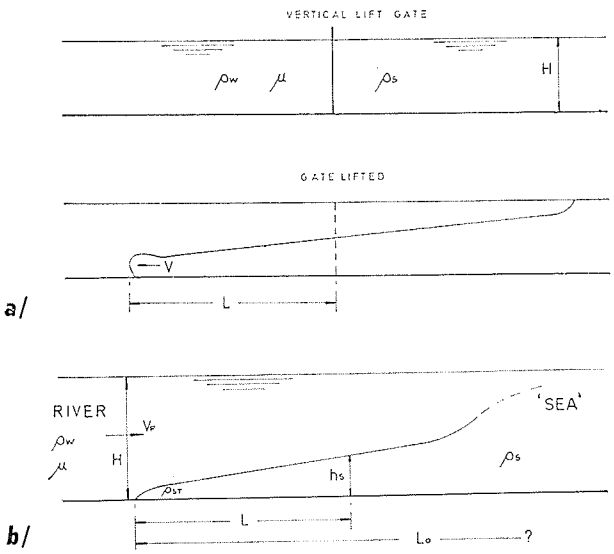

1/ Schematic representation of: *a*) lock exchange flow; *b*) arrested saline wedge.

Représentation schématique : a) *écoulement consécutif à l'ouverture d'une vanne;* b) *coin salé en régime permanent.*

* Dept. of Civil Engineering, University of Strathclyde, Glasgow.

included a theoretical treatment of the salt wedge within their more general "Theoretical Considerations of the Motion of Salt and Fresh Water".)

Arrangement of variables

Consider the idealised wedge system shown in figure 1 *b*, this system being contained within a horizontal, rectangular, prismatic channel of breadth B. A constant discharge of fresh water of density ρ_w and coefficient of viscosity μ enters the channel from the left hand or "river" end and flows along the channel towards the right hand or "sea" end. More dense salt water of density ρ_s is allowed to intrude from this end and penetrates upstream until arrestment. The overall depth of the water immediately in front of the stabilised wedge tip is given by H, V_F being the mean velocity of the less dense water at that point. Neglecting the effects of surface tension and any air/water surface waves, the foregoing six imposed variables, that is B, H, ρ_s, ρ_w, μ and V_F, are sufficient to define the system.

In this present paper interest is solely in the extent of the wedge penetration and thus the resultant variable showing the effect of change in any of the imposed variables will be chosen as some measure of length. It has been customary to take the resultant as the "overall" length, L_0, of the wedge from the channel mouth to the wedge tip, the sudden expansion at this point resulting in the underflow attaining critical conditions. Apart from the difficulty of creating a sudden expansion and extensive "sea" in large scale, wide channel, laboratory tests, natural channels generally do not terminate in abrupt increases in width and thus the point of critical depth, the accepted downstream limit of the wedge, is very difficult to define. For these reasons it was considered that the purpose of the tests, including the projection of the results to prototype conditions, would be better served if the resultant was chosen as the length L of the wedge measured from the tip downstream to some chosen wedge height h_s. With the reference point for the extent of penetration the wedge tip, the imposed salt water density should also be referred to this point, the value being given by ρ_{ST}. The resultant variable L can now be expressed as a function of the six imposed variables and h_s :

$$L = \Phi (\rho_{ST}, \rho_w, \mu, V_F, H, B, h_s) \qquad (1)$$

For effectiveness the terms of Equation (1) must be arranged into a form suitable for correlation, the most appropriate result for comparison of geometrically similar systems being an *n*-term, non-dimensional, functional equation. A first step in the obtaining of such an equation is the creation of a dimensional and explicitly dimensionally homogeneous equation of $(n + 1)$ terms. In the most simple arrested wedge system complete geometrical similarity could be achieved with the general length l as the unique linear size measure. The length l could be any one of the four defined size terms, L, H, B, h_s, the other three of which are now in constant proportion to each other. Using the single length term, two representative velocities can be defined as measures of the active forces within the considered system. Because of the difference in density between the salt and fresh water a gravitational accelerative velocity results, this being given by $g'_w{}^{1/2} . l^{1/2}$ where

$$g'_w = \frac{\rho_{ST} - \rho_w}{\rho_w} \cdot g$$

Because of viscous effects a retarding velocity also is relevant, this force measure being given by ν/l where ν is the kinematic viscosity coefficient equal to μ/ρ_w. A complete functional equation for the simplified system can now be obtained by the use of the two foregoing active force measures and by the imposed fresh water velocity V_F, the resultant variable being given by l:

$$\Phi (g'_w{}^{1/2} . l^{1/2}, \nu/l, V_F) = 0 \qquad (2)$$

By arranging the three possible ratios of the above three velocity terms (any two of which ratios are sufficient to define the three terms) to give the length l raised to the power one in the denominator, three linear ratios are obtained, any two of which are again sufficient to define the system:

$$\Phi \left(\underbrace{\frac{\nu^{2/3}}{g'_w{}^{1/3} . l}, \frac{\nu}{V_F l}, \frac{V_F{}^2}{g'_w . l}}_{\text{Any 2 of 3}} \right) = 0 \qquad (3)$$

On then taking the common length l out of each ratio a three term linear equation is obtained, this consisting of the length l and any two of three "linear proportionalities":

$$\Phi \left(\underbrace{\frac{\nu^{2/3}}{g'_w{}^{1/3}}, \frac{\nu}{V_F}, \frac{V_F{}^2}{g'_w}}_{\text{Any 2 of 3}} , \; l \right) = 0 \qquad (4)$$

Equation (4) can now be easily extended from the simplified system to that defined in Figure 1 *b* by the replacement of l by all of the four size terms:—

$$L = \Phi \left(\underbrace{\frac{\nu^{2/3}}{g'_w{}^{1/3}}, \frac{\nu}{V_F}, \frac{V_F{}^2}{g'_w}}_{\text{Any 2 of 3}} , H, B, h_s \right) \qquad (5)$$

The above equation is thus the most general expression of a six term dimensional and explicitly dimensionally homogeneous equation for the defined variables of Equation (1).

Choosing the terms $\nu^{2/3}/g'_w{}^{1/3}$ and $V_F{}^2/g'_w$, six terms of Equation (5) can now be transformed to one suitable five term non-dimensional functional equation :

$$L/H = \Phi \; [(\nu^{2/3}/g'_w{}^{1/3})/H, (V_F{}^2/g'_w)/H, B/H, h_s/H] \qquad (6)$$

or :

$$L/H = \Phi \; [g'_w{}^{1/2} . H^{3/2}/\nu, \; V_F/g'_w{}^{1/2} H^{1/2}, \; B/H, h_s/H]$$

or, with

$$\boxed{U = g'_w{}^{1/2} H^{1/2}}$$

$$L/H = \Phi \; [UH/\nu, V_F/U, B/H, h_s/H \qquad (7)$$

The first two groups on the right hand side of Equation (7) are respectively the densimetric Froude Reynolds number, now generally known as the Archimedes number, and the densimetric Froude number. Replacing L by L_0, the "overall" length of the wedge (and h_s/H therefore eliminated) Equation (7) is seen to be that derived by Keulegan [7] for his investigations of the arrested wedge.

Experimental arrangement

Experiments were undertaken in two rectangular, prismatic, horizontal, laboratory channels, one being for "small scale" and the other for "large scale" studies. The smaller

of the two channels was of perspex and was closed, the internal breadth and height being 10.16 cm and the available length 9.3 m. For the "large scale" studies, an open-topped steel channel was used. This channel was 87.5 m long and 1.52 m wide and a maximum water depth of 40 cm could be obtained. In order that tests could be carried out at varying relative channel breadth and yet retain maximum depths, an adjustable internal partition could be inserted over the length of this larger channel.

For the greater part of the investigation a sudden expansion in channel breadth was not provided and the traditional "sea" was replaced by a controlled inflow of salt water through an introduction box. That used with the 10.16 cm square sectioned channel is shown in Figure 2 *a*. Salt water entered at the base and the tight fitting, adjustable level deflection plate ensured that the egress would be into the channel. In the 1.52 m wide channel no expansion in depth was allowed and the introduction box shown in Figure 2 *b* was fitted on the channel bed close to the downstream end. The height of this introduction box was not adjustable but was fixed at half the overall depth of flow.

Assessment of salt introduction system

To examine the suitability of the arrangements adopted to simulate a "sea" and in particular to check the effect of variation in the rate of salt water input (this not having been taken as an imposed variable), a series of wedges were formed in the small channel with the values of overflow velocity, density difference, depth and temperature held constant but with varying salt water inputs. For these tests the deflection plate height was set at H/2. When each wedge became stabilised, its profile was recorded by measuring the height of the interface at increments of length and these profiles were first plotted with the introduction box as the common origin as shown in Figure 3 *a*.

Examination of the interfacial profile, firstly, of individual wedges, reveals that each consists of three distinct sections. Extending from the tip to a relative wedge height (for this series) of about 0.15 there is a section of decreasing interface curvature, the "nose" of the wedge, and this is followed by a section that is virtually a straight line. Near the introduction box there is a section of increasing curvature. The linearity of a considerable proportion of the interface length has not been commented upon by previous researchers but a study of such profiles as have been recorded [6, 9] shows that in all cases such linearity, or a very close approximation thereto, was obtained. Most theoretically derived wedge profiles contain a linear section.

Considering all five profiles of Figure 3 *a*, it is seen that the overall length of the wedge and its height at a given point increase with increase in the rate of salt water input until maximum values are reached beyond which increase in salt water input no longer affects the profile. By superimposing the profiles such that the tips are coincident, however, the chosen dependent variable, the length from the tip to some relative wedge height h_s, is seen to be unaffected by the rate of walt water input where h_s is within the upstream curvature or linear sections of the interface, Figure 3 *b*. Until the commencement of the downstream section of increasing curvature the wedge profiles are in all respects equal with only the length of the linear section affected by the rate of salt water input.

Similar series of tests were conducted to determine the

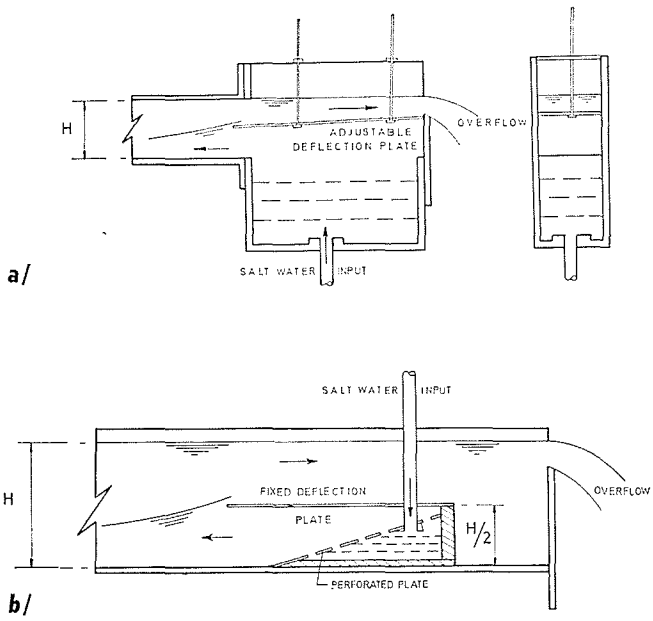

2/ Salt water introduction box used: *a*) with 10.16 cm square sectioned channel; and *b*) with "large scale" tests.

Boîte d'introduction d'eau salée employée : a) *avec un canal de section carrée de 10,16 cm;* b) *pour des essais à grande échelle.*

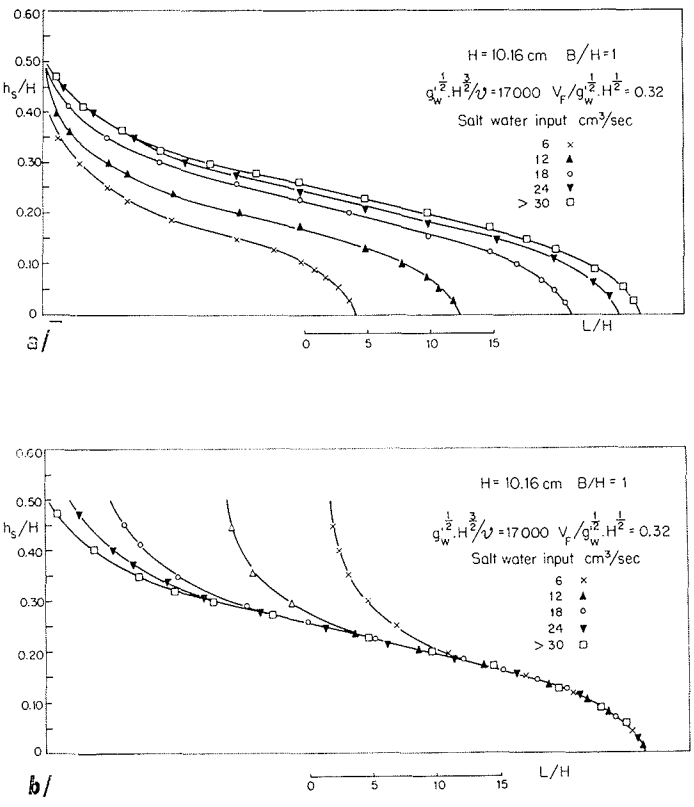

3/ Effect on wedge profile of variation in salt water inflow: *a*) profiles plotted with introduction box as common origin; *b*) profiles plotted with wedge tips coincident.

Influence de la variation du débit d'eau salée injecté sur le profil du coin : a) *boîte d'introduction représentant l'origine commune pour tous les profils;* b) *extrémités des coins coïncidant pour tous les profils.*

effect of variation in the deflection plate height for one rate of salt water input and again it was found that this did not affect the profile from the tip downstream to the point where linearity of the interface ceased. By combining the two foregoing arrangements wedges were then formed by varying both the salt water inflow and the deflection plate height. Similar results to those found previously were once more obtained. One particular advantage of this adjustment of inflow and deflection plate height was the ability to create "thin" wedges of low densimetric Froude number. This could be done with the knowledge that these accurately represented the upstream portion of a wedge of this densimetric Froude number precluded from being formed to the maximum values of h_s/H because of restrictions as to the available length of channel. Similar tests on the rate of salt input were undertaken with the large channel, with similar results, but for convenience the introduction box height was fixed at H/2 for these "large scale" tests.

Variation in densimetric Froude number

Having ascertained that the method of salt water introduction did not influence the chosen resultant variable so long as h_s was within the linear or upstream curved portions of the interface, examination of the effect of the imposed independent variables on the penetration could be made. Of the non-dimensional groups on the right hand side of Equation (7), firstly the effect of varying the ratio V_F/U was examined, with H, B/H and UH/ν held constant. This was achieved by varying the overflow velocity V_F. Figure 4 shows the profiles of the wedges obtained in one series of tests in the small flume with H = 10.16 cm, B/H = 1 and UH/ν = 17,000. As adjustment of salt input and deflection plate height was undertaken to enable low values of V_F/U to be obtained, comparison of overall lengths cannot be made, but by considering the length of the wedges from the tips to values of h_s/H up to the cessation of interface linearity at the downstream end, values of L/H can be obtained and plotted against V_F/U for the chosen values of h_s/H. This form of plot eliminates any distortion caused by the artificiality of the introduction. Figure 5 shows such a plot for h_s/H values ranging from 0.05 to 0.30 for the profiles of Figure 4 and demonstrates the increase in relative wedge length with decrease in overflow velocity, that is decrease in V_F/U, the densimetric Froude number. It is also seen that a change in overflow velocity at a low value of V_F/U has a greater effect on relative wedge length than a similar change at high values.

Variation in Archimedes number

To examine the effect on penetration of change in densimetric scale, series of wedges similar to those of Figure 4 were formed with each series of varying UH/ν. As the overall depth was still held constant at 10.16 cm this was achieved primarily by varying the density difference although small changes in temperature also contributed. Similar plots to that of Figure 5 were made for each value of UH/ν and the lines of constant h_s/H extracted from each for plotting on separate figures. That for the value $h_s/H = 0.25$ is shown as Figure 6. Each densimetric scale of tests is shown by a separate curve, the non-uniformity revealing that the underflow will penetrate further as the ratio of gravitational effects U, resulting from the density difference, to viscous effects, ν/H, becomes greater.

Variation in overall depth

That the effects of physical scale on the penetration might be examined, series of tests were undertaken in the large channel at three separate overall depths, H = 30.5 cm, H = 22.8 cm and H = 15.2 cm. For all three depths the internal partition was adjusted to maintain the relative breadth at unity and the experimental configuration kept geometrically similar, in particular the introduction box height at H/2. At each depth group of tests were carried out at values of UH/ν that included those common to at least one other depth and in the case of the 15.2 cm depth, at values common to those used in the 10.16 cm channel.

Figure 7 shows the variation in relative length with change in V_F/U and UH/ν for the tests with H = 30.5 cm while Figure 8 is a similar plot for one common value of UH/ν at H = 30.5 cm, 22.8 cm and 15.2 cm. From this figure it can be seen that the results obtained from the three different physical sizes of test in the large channel are not coincident, as might be expected for this value of UH/ν, there being an increase in relative length with increase in the overall depth of flow for all values of V_F/U. The wedges formed in channels of different physical size are not then geometrically similar and the tests in the channel of overall depth H = 15.2 cm did not result in "models" of those with H = 22.8 cm and 30.5 cm even although B/H, V_F/U and UH/ν were equal. For the correlation of Equation (7) therefore, that common to all studies of arrested saline underflows to date, freedom from all forms of scale effects appears not to have been achieved even for values of UH/ν up to 60,000.

Superimposed profiles

To investigate more closely the effects of physical size, densimetric size and overflow velocity on the wedge penetration, an examination was made of selected wedge profiles by superimposing them such that the $h_s/H = 0.25$ relative heights were coincident. Figure 9 *a* shows the profiles of a group of wedges having equal values of UH/ν and H but with differing values of V_F/U, that is varying overflow velocity. As shown by Figure 7, reduction in the value of V_F/U results in an increase in the relative length, but the form of plotting used in Figure 9 *a* reveals that this increase is achieved primarily by an increase in the length of the linear portion of the interface resulting from a decrease in the slope.

Figure 9 *b* shows a further set of profiles, these being for two groups of wedges of varying values of UH/ν, the constant values of V_F/U being 0.416 and 0.303. The overall depth H is again constant. As shown previously, again in Figure 7, increase in UH/ν for constant V_F/U results in an increase in the relative length of the wedge. The increase in the relative length, however, is now shown by Figure 9 *b* to be accounted for entirely by an increase in the length of the linear interface, this increase being achieved once more from a decrease in the slope but also

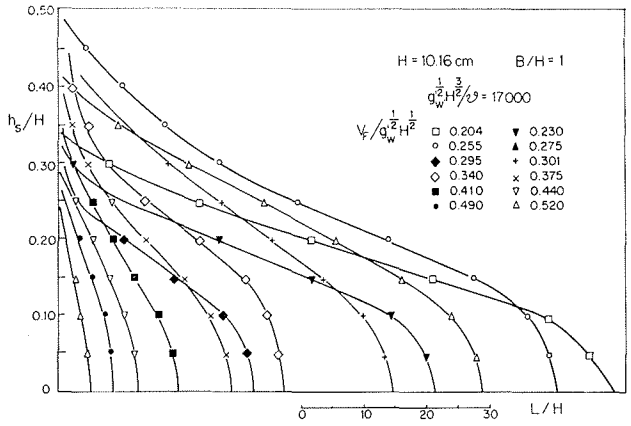

4/

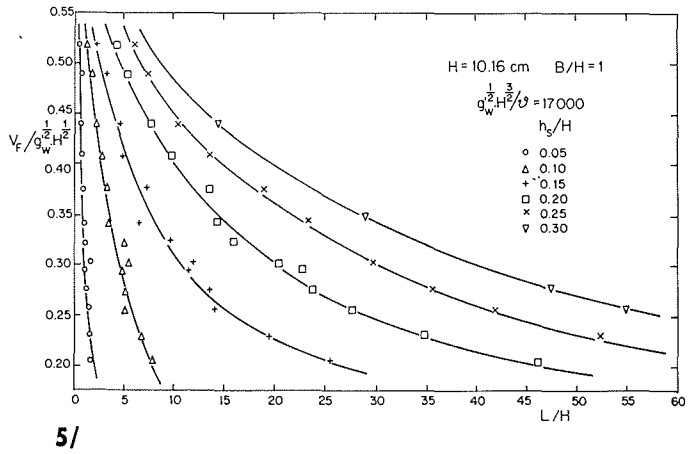

5/

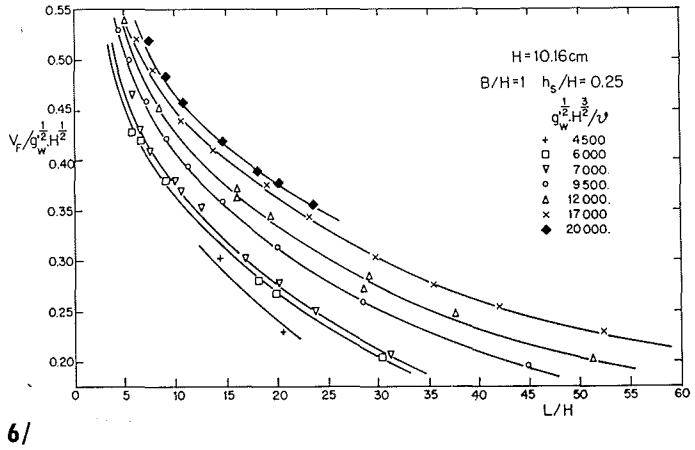

6/

4/ Variation in wedge profiles with change in densimetric Froude number.

Variation du profil du coin salé en fonction de la variation du nombre de Froude densimétrique.

5/ Variation in relative wedge lengths with change in densimetric Froude number.

Variation de la longueur relative du coin salé en fonction de la variation du nombre de Froude densimétrique.

6/ Variation in relative wedge length with change in Archimedes number. H = 10.16 cm.

Variation de la longueur relative du coin salé en fonction de la variation du nombre d'Archimède. H = 10,16 cm.

7/ Variation in relative wedge length with change in Archimedes number. H = 30.5 cm.

Variation de la longueur relative du coin salé en fonction de la variation du nombre d'Archimède. H = 30,5 cm.

8/ Effect on relative wedge length of change in overall depth of flow.

Influence de la variation de la hauteur globale de l'écoulement sur la longueur relative du coin salé.

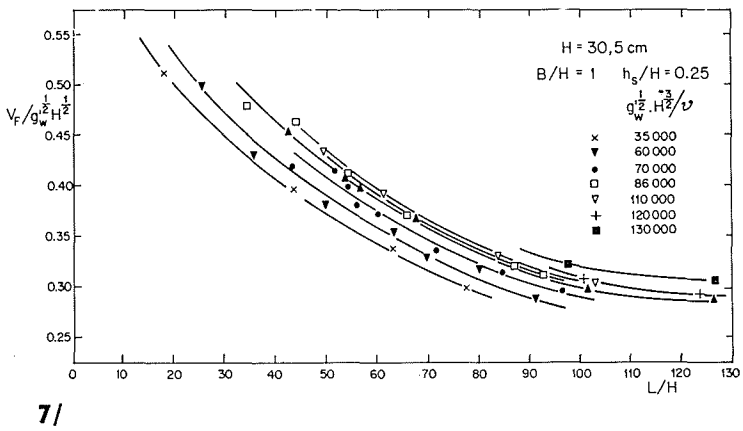

7/

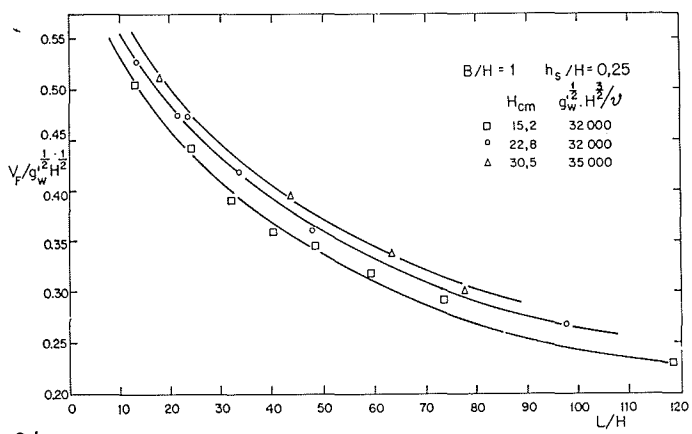

8/

from a decrease in the value of h_s/H at which the linear portion commences. In effect, as UH/ν increases, the wedge profile becomes more truly wedge shaped as the length of the nose reduces both actually, and as the proportion of the total relative length.

Figure 9 *c* shows three pairs of wedges, each pair having equal values of V_F/U and UH/ν but with varying values of overall depth H. Figure 8 revealed that an increase in the overall depth in such a situation resulted in an increase in the relative penetration of the wedge and by examining Figure 9 *c* it is seen that this increase is obtained solely from a lowering of the relative wedge height at which the linear portion of the interface commences. With V_F/U and UH/ν equal the slope of the linear parts of the interfaces are now equal, but because of the increased penetration of this part of the interface the relative length of the wedge nose occupies a lesser proportion of the total relative length. Thus, as the overall depth H is increased, the wedge becomes again more truly wedge shaped.

One explanation for the variation obtained in relative length with variation in overall depth could be the effect of the roughness of the channel sides and bed on the more sensitive wedge nose. Relative channel roughness was not considered as an imposed variable and the actual roughness remained the same for all water depths. On examining all the wedge noses it became apparent that the actual shape of the nose, that is the actual length to the point, and height at the point, where curvature ceased, was approximately equal for equal values of V_F/U and UH/ν irrespective of the overall depth of flow. When the relative shape of the nose is considered, the nose is reduced in longitudinal and vertical extent with increase in overall depth and decrease in the relative roughness. For one value of actual channel roughness therefore, the wedge

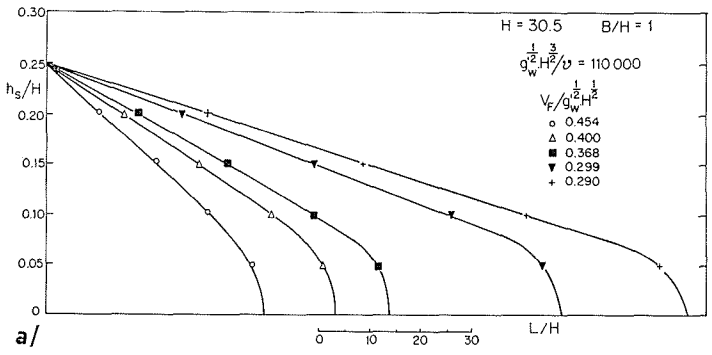

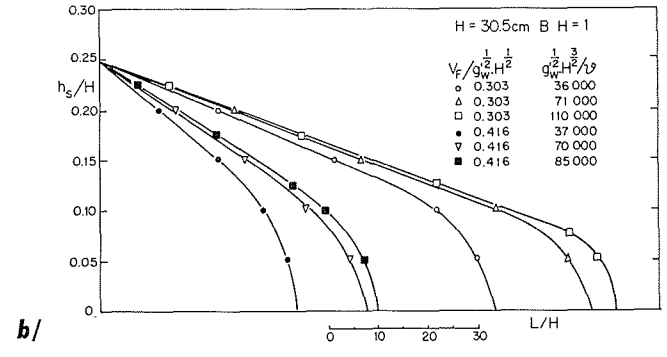

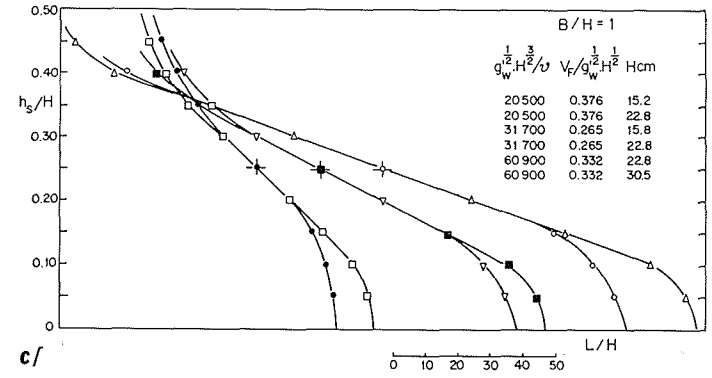

9/

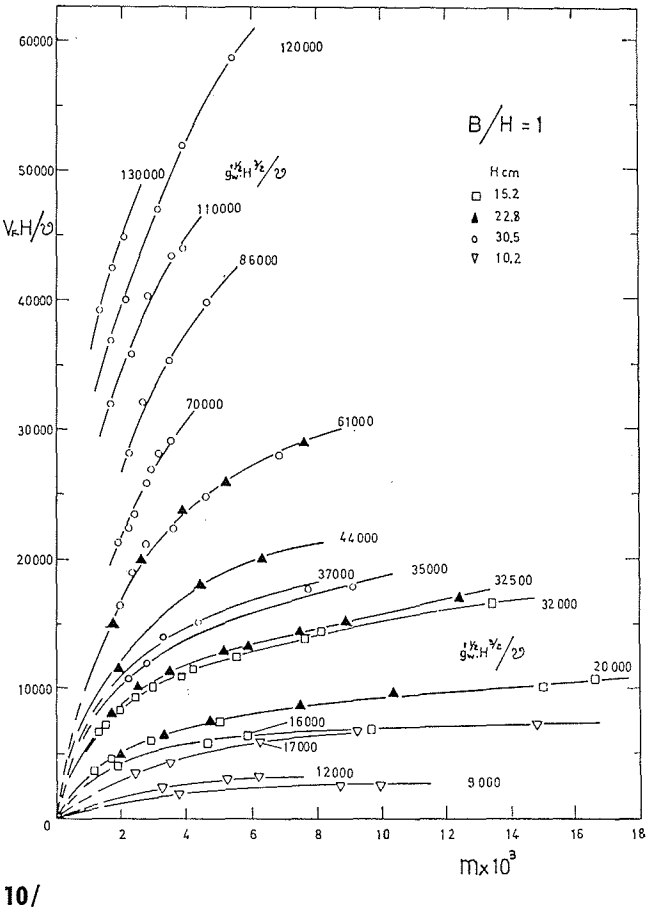

9/ Interface profiles superimposed with $hs/H = 0.25$ relative wedge heights coincident: *a*) variation in densimetric Froude number; *b*) variation in Archimedes number; *c*) variation in overall depth of flow.

Superposition des profils de l'interface avec $hs/H = 0{,}25$ *et coïncidence des hauteurs relatives du coin :* a) *variation du nombre de Froude densimétrique;* b) *variation du nombre d'Archimède;* c) *variation de la hauteur globale de l'écoulement.*

10/ Variation in interface slope with change in Reynolds number and Archimedes number, $B/H = 1$.

Variation de la pente de l'interface en fonction de la variation des nombres de Reynolds et d'Archimède, avec $B/H = 1$.

tends to become more truly wedge shaped with increase in overall depth as the relative size of the nose is reduced.

Slope as resultant variable

The greatest proportion of a change in relative wedge length results from a change in the slope of the linear portion of the interface and it has been shown that as the densimetric and physical size of a wedge is increased the linear portion of the interface extends closer to the wedge tip for one value of channel roughness. In addition, the slope of the linear portion of the interface, unlike the total relative length, has been shown to vary only with variation in $V_F/\mathbf{U}$ and $\mathbf{U}H/\nu$ for one relative breadth and to be free of scale effects at low values of Archimedes number. A more suitable dependent variable for examining wedge penetration might then be the slope of the linear portion of the interface. A further reason for the use of slope rather than relative length, is the variation caused in the latter by channel bed irregularities, for preliminary results obtained by the author, together with those of Hinwood [12], suggest that a rise in channel bed level of as little as 2 % of the overall depth may alter the wedge tip position by several depth lengths. The slope of the interface dowstream is unaffected, however, by such an irregularity.

A more effective plot might also be obtained if the densimetric Froude number was replaced in the n term functional equation by the Reynolds number of the overflow at the wedge tip. With the resultant variable as m, the slope of the interface at some relative height h_s/H, the functional equation is now :

$$m = \Phi\ [(\nu^{2/3}/g'_w{}^{1/3})/H,\ H/(\nu/V_F),\ B/H,\ h_s/H] \quad (8)$$

or :

$$m = \Phi\ [\mathbf{U}H/\nu,\ V_F.H/\nu,\ B/H] \quad (9)$$

with h_s/H omitted where m is the slope of the linear portion of the interface. The three terms on the right hand side of Equation (9) are respectively the Archimedes number, the Reynolds number and the relative channel breadth.

Using the groups of Equation (9), a plot can now be prepared showing the variation in interface slope with change in $V_F.H/\nu$ and $\mathbf{U}H/\nu$ for the relative breadth $B/H = 1$. Figure 10 shows such a plot for all the results obtained with $B/H = 1$ including those obtained with the "small scale" studies in the 10.16 cm closed channel. By using interface slope as the resultant variable it is seen that consistent results have been obtained for all the wedges formed in the "large scale" channel, wedges of equal $V_F.H/\nu$ and $\mathbf{U}H/\nu$ having the same interface slope irrespective of individual or collective variation in the independent variables ρ_{ST}, ρ_w, H, V_F, ν, and B. Physical, densimetric and temperature forms of scale effect have therefore been eliminated with the "large scale" tests.

The very low values of interface slope obtained, less than eighteen minutes of arc for most wedges, and the extreme sensitivity of the interface slope to changes in $V_F.H/\nu$ and $\mathbf{U}H/\nu$ is to be noted, the sensitivity being apparent with the use of Reynolds number as ordinate in a manner not obtained with the use of densimetric Froude number.

The results from the tests in the 10.16 cm square channel conform well amongst themselves but do not coincide exactly with the "large scale" results having similar values of $\mathbf{U}H/\nu$. This could suggest that some form of scale effect was becoming apparent as Archimedes number, the measure of "scale," decreased but is more likely to be a result of the small 10.16 cm channel being closed. An air/water interface was not present when the relative breadth was unity in this channel and thus the velocity distribution of the less dense water approaching the wedge and flowing over it was changed. With the maximum velocity of the overflow being nearer the channel bed (and hence the underflow) in the closed channel, salt water penetration was not so great and the interface slope was thus increased even although the values of $V_F.H/\nu$ and $\mathbf{U}H/\nu$ were equal.

Variation in relative channel breadth

To investigate the effect on wedge penetration of the third group on the right hand side of Equation (9), that is the relative channel breadth B/H, systematic series of tests were undertaken over a wide range of B/H values. Using H = 30.5 cm or 15.2 cm, values of 0.5, 5 and 10 were obtained in the larger channel while with H = 5.1 cm a value of 2 was obtained with the 10.16 cm channel. In addition tests were undertaken in a third open channel with an overall depth H of 7.6 cm and an available length of 6.2 m. Relative breadths of 1 and 5 were obtained with this channel. At each value of relative breadth in the large channel, tests were undertaken with values of $\mathbf{U}H/\nu$ that were common to at least one other relative breadth.

The profiles of the wedges formed in the channels of varying breadth again contained a distinct linear section and the variation in penetration with change in $V_F.H/\nu$ and $\mathbf{U}H/\nu$ was of a similar form to those having $B/H = 1$. As suggested by Keulegan [9], increase in the relative channel breadth of wedges having similar values of H, $V_F.H/\nu$ and $\mathbf{U}H/\nu$ was found to result in an increase in the penetration of the wedge. By superimposing profiles, this increase in length was shown to be achieved primarily by a reduction in the slope of the linear portion of the interface, wedges formed in wide channels having a linear interface of lesser slope than those formed in narrow channels, even although $V_F.H/\nu$, $\mathbf{U}H/\nu$ and H were alike. Plots similar to that of Figure 10 were prepared for each value of B/H investigated but for convenience it would be desirable if all values of relative breadth might be incorporated onto one diagram.

Use of hydraulic radius

It was considered possible that by including R, the hydraulic radius or hydraulic mean depth of the channel, as an imposed variable incorporating B and H and replacing either in certain groups, that such a single plot might result. The Archimedes number, $\mathbf{U}H/\nu$ is a group giving a measure of the ratio of the active accelerating force causing the underflow to penetrate upstream to the active viscous resistance force offered to it. The penetrating driving force depends only on the overall depth of flow H and the effective gravitational acceleration g'_w, and H is thus rightly used as the linear term associated with g'_w. Resistance to penetration, however, in addition to occurring

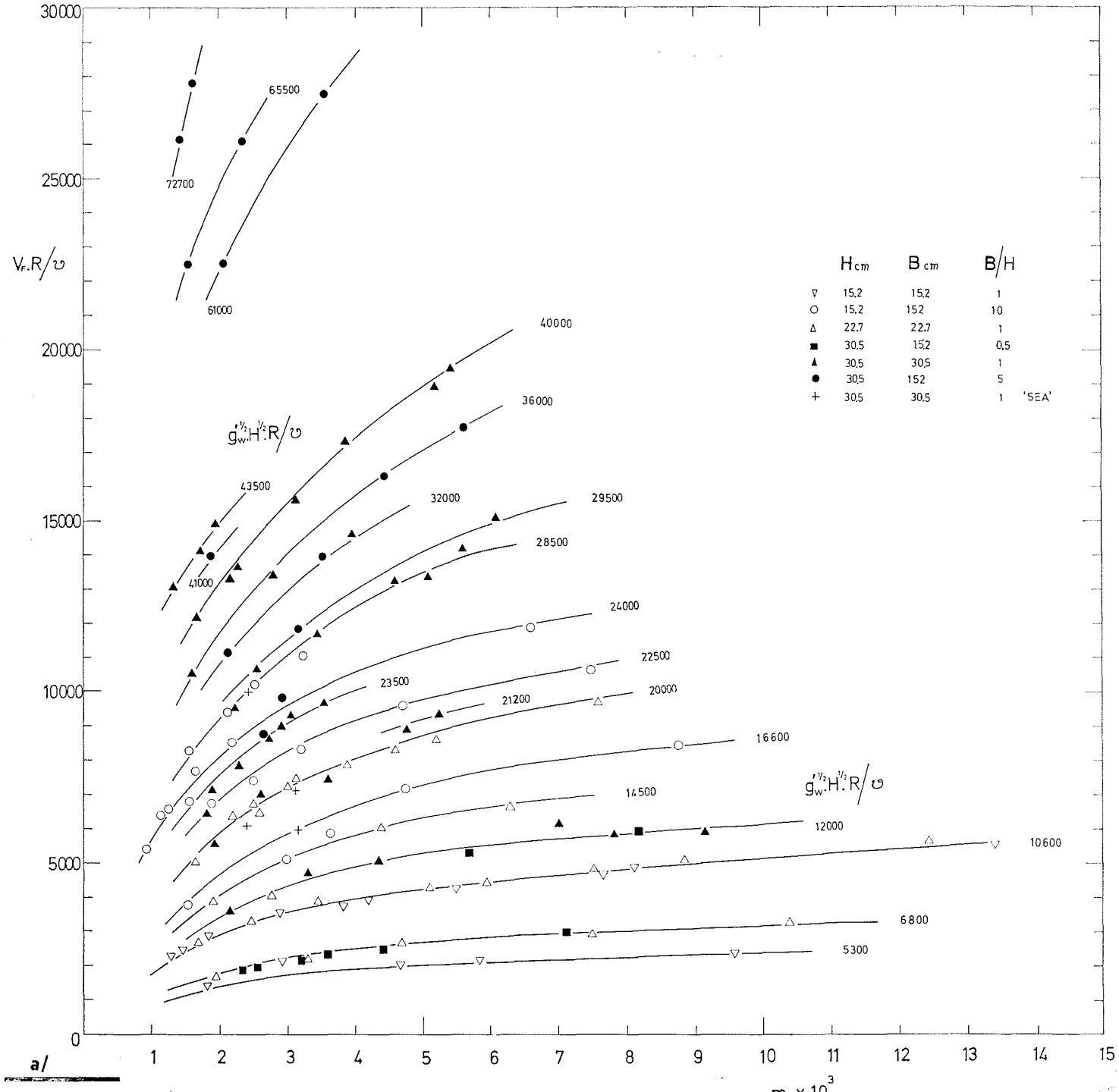

a/

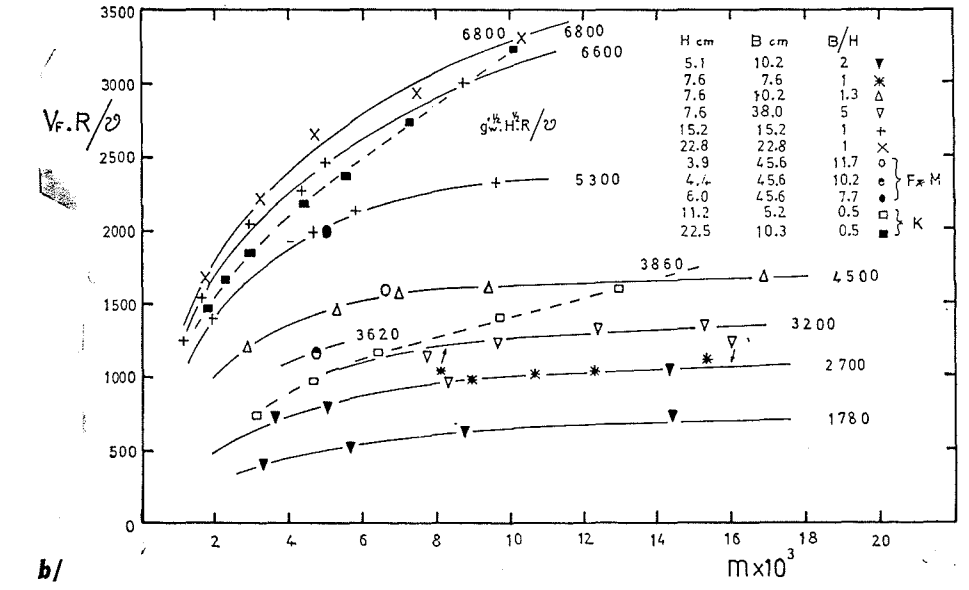

b/

11/

Variation in interface slope with change in Reynolds number and Archimedes number. All values B/H. *a*) "large scale" tests; *b*) "small scale" tests.

Variation de la pente de l'interface en fonction de la variation des nombres de Reynolds et d'Archimède, pour toutes valeurs de B/H : a) *essais « à grande échelle »*; b) *essais « à petite échelle ».*

along the interface also occurs along the channel bed and sides and it is thus logical that some account should be taken of the wetted perimeter of the channel in deriving the active resistance force measures. The hydraulic radius :

$$R = \frac{\text{Area of channel}}{\text{Wetted perimeter of channel}} = \frac{B.H}{B + 2H}$$

will therefore be used as the linear term in groups giving a measure of force actions opposing penetration while the overall depth H will be retained in groups giving a measure of force actions causing penetration. On this basis the non-dimensional equation may be rewritten as :-

$$m = \Phi\,[\mathbf{U}/(\nu/R),\ V_F/(\nu/R),\ R/H] \qquad (10)$$

or :

$$m = \Phi\,[\mathbf{U}R/\nu,\ V_F.R/\nu] \qquad (11)$$

with R/H only being retained where necessary for geometric similarity in modelling. Such a use of R in place of H was suggested by Barr in the third paper in this series [3] and was used by him in a recent discussion [14] to explain results obtained by Keulegan. Wu [15] has also applied the concept of hydraulic mean depth to density currents, his rearrangement of Keulegan's results for exchange flow and wedge length appearing simultaneously with Barr's.

Figure 11 *a* shows the results of all the tests undertaken in the large flume with relative breadths of 0.5, 1, 5 and 10 plotted on the basis of Equation (11). Complete equality of interface slope for equal values of $V_F.R/\nu$ and $\mathbf{U}R/\nu$ has now been obtained with tests of all four relative channel breadths and interface slope is thus shown to be dependent solely upon the overflow Reynolds number at the wedge tip and upon the Archimedes number of the exchange. Equation (11) is therefore a completely effective correlation for the arrested saline underflow where the measure of penetration is taken as the interface slope. Again the great sensitivity of the slope of the linear interface to changes in $V_F.R/\nu$ and $\mathbf{U}R/\nu$ is apparent, variation in slope occurring with changes in the latter of as little as 1 %.

To examine the results of the "small scale" tests, that is tests with values of $\mathbf{U}R/\nu$ below about 10^4, a plot similar to that of Figure 11 *a* was prepared. This is shown as Figure 11 *b* and included on this plot are tests with B/H = 1 and H = 15.2 cm obtained in the large channel and tests with B/H = 2 and H = 5.1 cm undertaken in the 10.16 cm channel. Results of tests in the small channel with B/H = 1, H = 10.16 cm, are not included because of the differing velocity distribution in these tests due to the closed top. The agreement of results on this "small scale" diagram is not so satisfactory as with Figure 11 *a* showing that scale effects are apparent at these lower values of Archimedes number.

Check on experimental configuration

It was thought very unlikely that the substitution of an introduction box for the "sea" would have any effect on the characteristics of the wedge formed upstream in the channel except perhaps for that part of the wedge close to the introduction, that is the downstream section of increasing curvature. To ensure that this was the case and that the results obtained from the wedges based on an introduction box were applicable to those based on a conventional "sea," some tests were run in the large channel with a "sea" at the downstream end. For a channel of depth H = 30.5 cm and a relative breadth of unity the "sea" was created by allowing an expansion in breadth to B/H = 5. This sudden expansion had a length of 15 m (that is a relative length of 50) between the channel "mouth" and the overflow weir.

Because of the considerable time and expense required for this method of wedge formation only five penetrations were created using the "sea," the profiles of two of which are shown in Figure 12. From these profiles it is seen that the linear portion of the interface occupies some 73% of the overall length of the wedge from channel "mouth" to wedge tip while the upstream nose section occupied just over 8%. Thus even for this "size" of wedge, $\mathbf{U}R/\nu = 28{,}000$, definition of the interface slope allows a reasonable determination of the overall penetration to be made. The slopes of the wedges based on the "sea" are shown plotted on Figure 11 *a* and are seen to conform exactly with the results obtained from the tests using the introduction box. This clearly shows that the portion of the wedge extending upstream from the cessation of the linear portion of the interface at the downstream end is

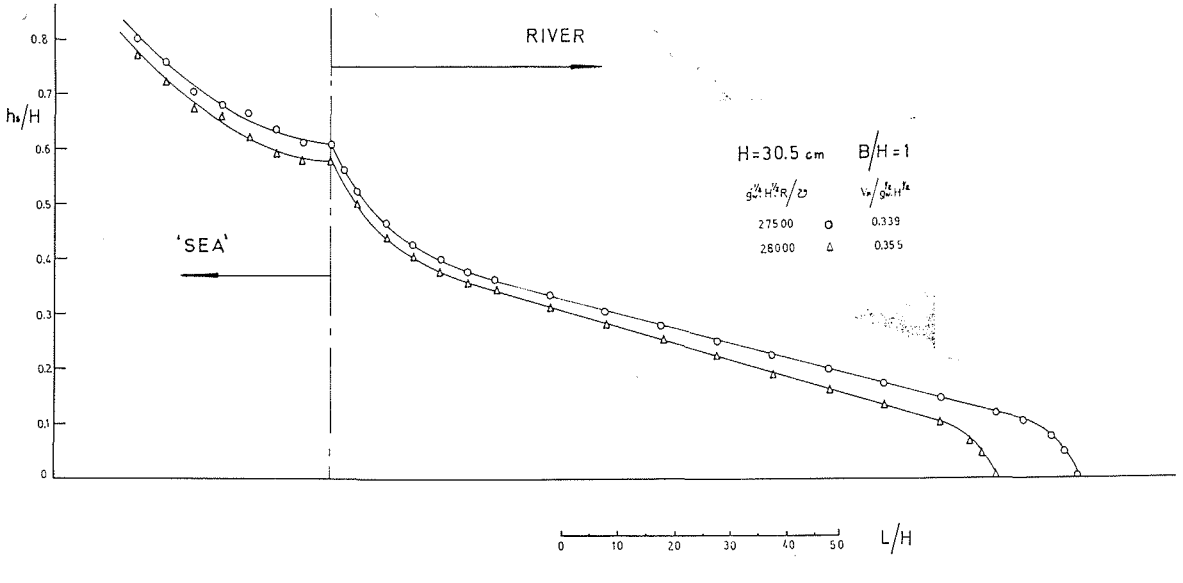

12/

Interfacial profile of wedges formed in channel leading from a "sea".

Profil d'interface des coins se formant dans un canal débouchant d'une «mer».

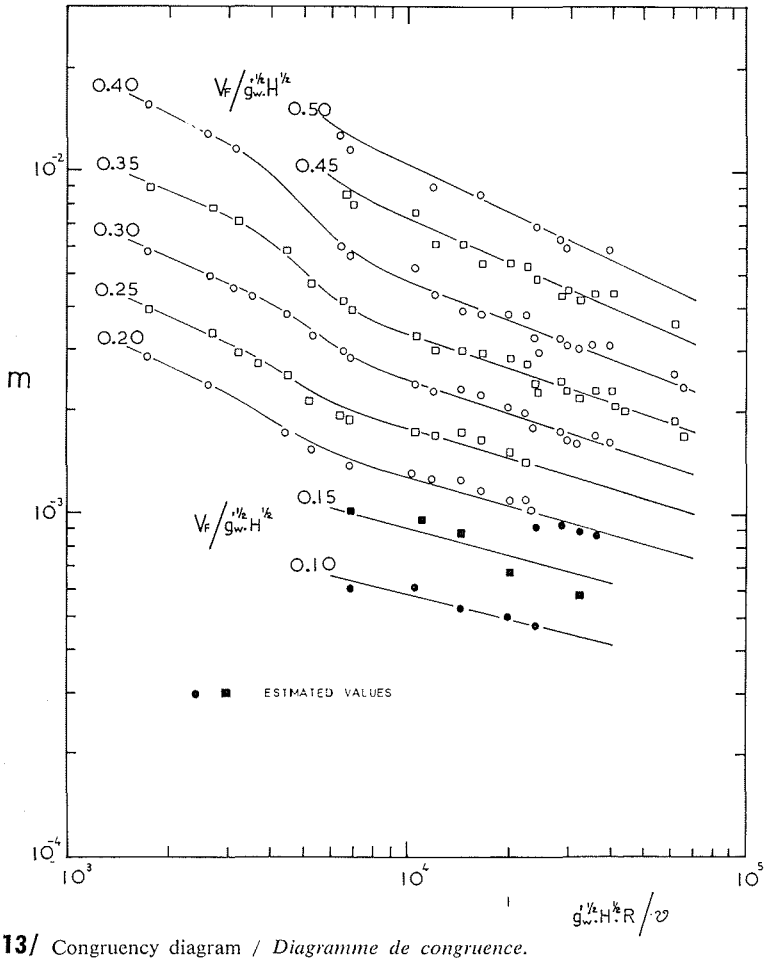

13/ Congruency diagram / *Diagramme de congruence.*

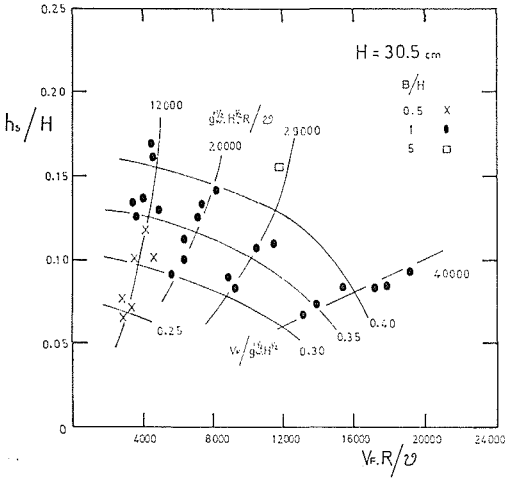

14/ Variation in value of relative wedge height at which linear portion of interface commences with change in densimetric Froude number and Archimedes number, H = 30.5 cm.

Variation de la valeur de la hauteur relative du coin salé correspondant au début de la partie linéaire de l'interface, en fonction de la variation des nombres de Froude densimétrique et d'Archimède, avec H = 30,5 cm.

not affected by the "sea" or the artificial representation thereof.

Profiles of two series of Keulegan's tests [9, 16] having a relative channel breadth of 0.46 were also examined. These tests were formed in a channel leading from a "sea" but it was unfortunate that the density differences employed in the respective series examined were the rather extreme values of 0.0046 and 0.113. For the eleven profiles examined the linear portion of the interface was found to occupy about 75% of the overall length with the former density difference and about 65% with the very high value. Keulegan's results are shown plotted on Figure 11 *b*. While they conform generally, agreement is not complete, it being likely that the combination of a narrow channel with extreme density difference, and in one case low depth, results in scale effects differing from those affecting the author's "small scale" studies. Some results obtained from profiles published by Farmer and Morgan (6) for wide but again "small scale" tests, are also included on Figure 11 *b*.

Congruency diagram

For the results shown in Figures 11 *a* and 11 *b* to be applied to prototype conditions, they must be expressed in a form that enables projection to higher values of $\mathbf{UR}/\nu$ to be made while ensuring that the results obtained from such a projection are similar to those used for the projection. The most effective form of plot suitable for these purposes is the congruency diagram with Archimedes number, the measure of "scale," as abscissa. For the standard congruency diagram relating to rate of spread [3, 17] freedom from all forms of scale effect is indicated by the non-dimensional rate of spread becoming equal with increase in the value of Archimedes number, the plotted points tending to a straight line which can be projected to values of Archimedes number greater than those obtainable in the laboratory.

To obtain a congruency diagram for the arrested saline underflow, lines of constant $V_F/\mathbf{U}$ were superimposed on Figures 11 *a* and 11 *b*, the values of $V_F/\mathbf{U}$ being taken at increments of 0.05. The values of m obtaining where these lines intercepted the lines of constant $\mathbf{UR}/\nu$ were then plotted against Archimedes number for each value of densimetric Froude number. Figure 13 shows the resulting plot, a logarithmic scale being used for convenience. Allowing for minor, unsystematic variations, a single line can be drawn through all the points for each value of $V_F/\mathbf{U}$ and from a value of $\mathbf{UR}/\nu$ greater than about 7×10^3, these lines become straight, and continue straight, until the maximum value of $\mathbf{UR}/\nu$, 6.5×10^4, obtained in the laboratory. There is thus no reason to suppose that the lines cannot be projected to higher values of $\mathbf{UR}/\nu$. For values of $\mathbf{UR}/\nu$ less than 7×10^3 the lines are not straight and can be considered only to be approximate, for while a value of $\mathbf{UR}/\nu$ derived from differing combinations of g'_w, H and ν gives a similar resultant, variation in relative channel breadth, or hydraulic mean radius, causes some variation in m at the lower values of Archimedes number.

Definition of linear interface

In addition to knowledge of the slope of the straight line portion of the wedge interface, some knowledge of the relative wedge heights at which this linear portion commences and ceases must also be available for the prediction of wedge penetration. Considering firstly the value of h_s/H at the upstream, or nose end, this has been shown to be affected by the Archimedes number, the densimetric Froude number, and possibly by the relative roughness of the channel bed and sides. A comprehensive examination of roughness was not made and so results from only one overall depth, that is H = 30.5 cm, will be considered. By taking the value of h_s/H at which the linear portion of the interface commenced at the upstream end from the recorded wedge profiles, a plot can be made of these values of h_s/H against the corresponding values of $V_F R/\nu$ for the values of UR/ν. This plot is shown as Figure 14 for $V_F R/\nu$ up to 2×10^4. Lines of constant V_F/U are superimposed upon this diagram.

As suggested by Figures 9 *a* and 9 *b* the value of h_s/H at which the linear portion of the interface commences increase with increase in $V_F R/\nu$ for each value of UR/ν and decreases with increase in UR/ν for each value of V_F/U. As for one channel roughness h_s/H also decreases with increase in overall depth H, the results suggest that for a wedge of high value of Archimedes number and of relatively low, that is less than 0.35, value of densimetric Froude number formed in a deep, smooth, channel, the value of h_s/H at which linearity of the interface commences will be low and probably in the range 0.05 — 0.07. Because of difficulty in determining the exact values of h_s/H from the test results, however, Figure 14 should only be taken as a general guide to the upstream h_s/H value. From the examination of the wedge noses it was also found for all values of $V_F R/\nu$ and UR/ν that the tip of the wedge stabilised at a distance upstream of the point where linearity of the interface commenced equal to one third to one half of the distance between that point and the point where a continuation of the linear interface would intercept the channel bed, Figure 15.

Unlike the upstream limit of interface linearity, the value of h_s/H at the downstream limit was unlikely to be affected by relative channel roughness and thus to be independent of the overall depth H. All depths could therefore be considered. The relevant value of h_s/H was obtained again from the recorded profiles for those wedges where the salt input was sufficient to cause maximum penetration for the values of $V_F . R/\nu$ and UR/ν obtaining. The values of h_s/H were then plotted against the densimetric Froude number, V_F/U, as shown in Figure 16. From this plot it would appear firstly that the value of h_s/H at which linearity ceases is independent of the overall depth of flow H and secondly that it is independent of the Archimedes number for, although scatter exists, this is random and unsystematic for both H and the Archimedes number. While a slight increase in h_s/H results with increase in relative channel breadth for each value of V_F/U, this is not large enough to be significant and a single best straight line was therefore drawn through all the points. The equation of this line is of the form :

$$h_s/H = 0.73 - 1.3\,(V_F/U) \qquad (12)$$

(with $U = g'^{1/2} H^{1/2}$)

That is the value of relative wedge height at which linearity ceases is solely a function of the densimetric Froude number of the flow at the wedge tip. For no wedge penetration, that is h_s/H reduced to zero, Equation (12) gives a value of V_F/U equal to 0.59. This compares with Keulegan's value of 0.75.

Longitudinal density variation

The adopted similitude arrangement required that the value of density applicable to the underflow be taken as that obtaining at the tip of the wedge. In order that this could be related to "sea" density and to underflow densities obtaining between the tip and the "sea," an investigation was made of the longitudinal variation in density within the wedge. The values of density were expressed as a percentage rise in density over the value at the tip, ρ_{ST}. It was found that the density within the wedge, near the channel bed, was approximately constant and only a very slight increase was apparent towards the "sea". Values of $[(\rho_S - \rho_{ST})/\rho_{ST}] \times 100$, with ρ_S the "sea" or salt input density, for the wedges showed that neither the value of densimetric Froude number nor the value of Archimedes

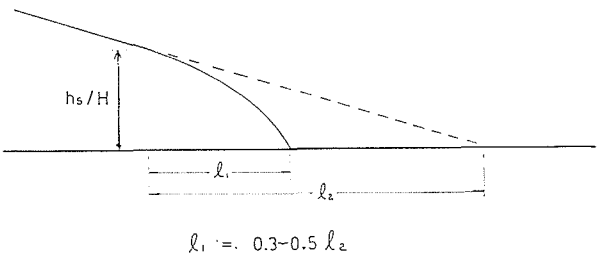

15/ Approximate position of wedge tip relative to value of *hs*/H at which linear portion of interface commences.

Position approximative de l'extrémité du coin par rapport à la valeur de hs/*H correspondant au début de la partie linéaire de l'interface.*

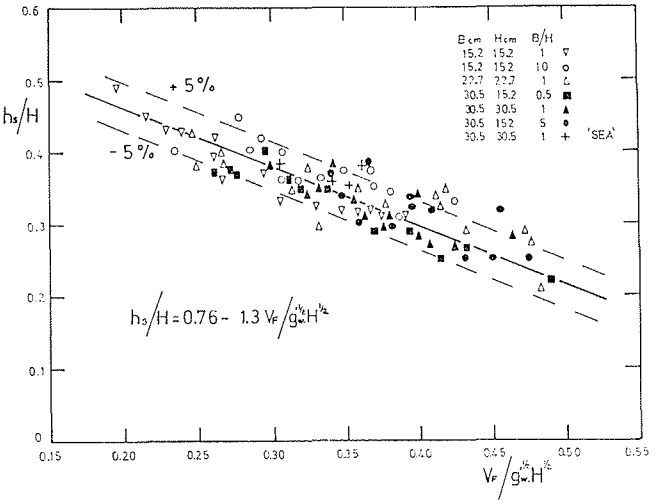

16/ Variation in value of relative wedge height at which linear portion of interface ceases with change in densimetric Froude number. All values B/H.

Variation de la valeur de la hauteur relative du coin correspondant à la fin de la partie linéaire de l'interface, en fonction de la variation du nombre de Froude densimétrique pour toutes valeurs de B/H.

number, UH/ν, affected the internal density variation. Any change in density was therefore independent of the length of the wedge. Slight variation in the value of $[(\rho_S - \rho_{ST})/\rho_{ST})] \times 100$ was apparent with change in relative breadth, however. As relative breadth decreased the change in density difference over the wedge length increased, the change occurring in that part of the wedge where the height was low, that is the part close to the tip. Values of mean percentage density change for the four relative channel breadths in the large channel are shown in table 1.

Table 1

B/H	MEAN VALUE $\frac{\rho_S - \rho_{ST}}{\rho_{ST}} \times 100$
0.5	3.5
1	1.7
5	1.0
10	0.8

The results suggest that any dilution occurring within the wedge is caused by mixing at the sides of the channel, mixing at the interface not being sufficient to cause dilution for any great depth below it. In a wide, smooth channel the density of the underflow close to the tip near the channel bed can be taken therefore as similar to that of the supplying "sea" and even in narrow channels the change is sufficiently small for the density of the wedge at the tip or in any part of its length to be taken as again that of the "sea".

Use of results

Knowledge of the breadth and overall depth of flow in a channel, the mean velocity of the less dense flow upstream of the wedge tip, the temperature and density of the less dense flow and the density close to the channel bed in any length of the wedge, allows the apposite values of UR/ν and V_F/U to be calculated. Figure 13 can then be entered at the value of UR/ν and the slope of the linear portion of the interface determined for the value of V_F/U. By taking one measurement of relative wedge height within the channel, ensuring that $h_s/H < 0.76 - 1.3\ V_F/U$, the length of the penetration from this point to the intercept of the projection of the linear interface with the channel bed can be found. For wedges of high, that is prototype, values of Archimedes number formed in a wide, smooth channel, this point of interception will closely approximate to the position of the wedge tip. For lower "model," values of UR/ν, reference to Figure 14 will enable the upstream limiting value of h_s/H to be estimated and the length to this relative height can then be calculated. Figure 15 gives an approximate guide to the position of the wedge tip relative to the upstream limiting value of h_s/H.

For one size of smooth, prismatic, rectangular and horizontal laboratory channel ending in a distinct, sudden expansion in channel breadth, the "overall" extent of wedge penetration from this sudden expansion to the wedge tip is a suitable resultant variable. The "overall" length is only of use, however, in such a situation, for when the limits between which it is measured are either indefinable or vary other than with variation in the imposed variables, the "overall" length is unpredictable. The upstream limit of the underflow penetration, the wedge tip, appears to be particularly sensitive to channel roughness and to small irregularities on the channel bed such as steps or shoals and the position of the tip, together with the extent of the curved nose, may vary from channel to channel even although the imposed groups of the functional equation remain constant. It is likely indeed that the shape of the wedge nose will be unique for each channel.

The Mississippi River, the classic example of a salt wedge estuary, has been shown to have an "overall" penetration of fourteen miles with H = 13.6 m and B/H = 33 [9]. The densimetric Froude number V_F/U for this penetration is 0.275 and the Archimedes number, UR/ν, is 2.1×10^7. Reference to a projection of the congruency diagram, Figure 13 gives a slope of 2.2×10^{-4} for these values. For a wedge with Archimedes number of 2.1×10^7 formed in a channel of similar characteristics to the large laboratory channel it would be expected that the extent of the wedge nose would be very small.

A recorded profile of the Mississippi, however, shows [10] the upstream limit of interface linearity as being a relative wedge height of about 0.25 and it is suggested that this is due in the main part to the irregularity of the channel sides and bed. The slope of the linear portion of the interface, which extends to a value of h_s/H at the downstream end considerably in excess of that given by Equation (12), is about 2.7×10^{-4}. While the experiments would result in some error in the estimated penetration of the prototype, the interface slopes are reasonably similar.

In addition to prototype prediction, the results allow effective correlation of varying laboratory tests and it is possible that their use might also be extended to prototype situations of low Archimedes number, for example gas or water vapour wedges arrested in mine passages and galleries.

Conclusions

Both the "small scale" and "large scale" tests described have demonstrated that a considerable proportion of the interface of an arrested saline underflow can be very closely approximated to a straight line and that such linearity is not affected by the normal imposed variables of a prismatic, horizontal and rectangular channel. The substitution of a "sea" by an introduction box, thus allowing greater relative channel breadths, has been shown to result in wedges that are in all dimensional respects similar to those obtained where a sudden expansion in breadth was included, except for a short length close to the introduction.

The difficulty of defining a downstream limit for the penetration has suggested the use of firstly, relative length from the tip as a measure of penetration and this relative length has been shown to increase with decrease in densimetric Froude number and to increase with increase in Archimedes number.

For one channel roughness, change in the overall depth of flow, all other groups being equal, has been shown to cause a variation in lengths measured either to or from the tip. Change in the slope of the linear portion of the interface has been demonstrated as being the prime component of length changes and also to be free of scale effects resulting from change in depth, density difference, temperature or channel breadth for a wide range of values of Archimedes number.

A congruency diagram has been prepared based on the hydraulic mean depth of flow that enables interface slope to be predicted and suggestions made as to the limits of the linear interface. It has been proved that no appreciable change in density occurs over the length of the underflow.

Acknowledgements

Financial support for this investigation was provided by the Science Research Council and the author is grateful to this body for its help and to the Clyde Port Authority for laboratory accommodation. Thanks are also due to Messrs. D. Burgess, T. Malcolm and J. Forbes who assisted with the experiments and to Professor D.I.H. Barr, author of the previous papers in this series, for his very helpful discussions.

References

[1] BARR (D. I. H.). — Densimetric exchange flow in rectangular channels. I: Definitions, review and relevance to model design. *La Houille Blanche*, No. 7 (November, 1963), 739-754.

[2] BARR (D. I. H.) and HASSAN (A. M. M.). — Densimetric exchange flow in rectangular channels. II: Some observations of the structure of lock exchange flow. *La Houille Blanche*, No. 7 (November, 1963), 757-766.

[3] BARR (D. I. H.). — Densimetric exchange flow in rectangular channels. III: Large scale experiments. *La Houille Blanche*, No. 6 (November, 1967), 619-632.

[4] PRITCHARD (D. W.). — Estuarine circulation patterns. *Proc. Amer. Soc. of Civil Engs.* Paper 717 (June 1955).

[5] FARMER (H. G.). — An experimental study of salt wedges. *Woods Hole Oceanographic Institution Technical Report*, Reference No. 51-99 (1951).

[6] FARMER (H. G.) and MORGAN (G. W.). — The salt wedge. *Woods Hole Oceanographic Institution Contribution*, No. 638 (1952). Or *Proc. 3rd Conference on Coastal Eng.*, Cambridge, Mass. (1952).

[7] KEULEGAN (G. H.). — Unpublished report: Interface mixing in arrested saline wedges. *U.S. Dept. of Commerce*, Nat. Bureau of Standards, Report No. 4142 (1955).

[8] KEULEGAN (G. H.). — Unpublished report: Significant stresses of arrested saline wedges. *U.S. Dept. of Commerce*, Nat. Bureau of Standards, Report No. 4267 (1955).

[9] KEULEGAN (G. H.). — Unpublished report: Form characteristics of arrested saline wedges. *U.S. Dept. of Commerce*, Nat. Bureau of Standards, Report No. 5482 (1957).

[10] SANDERS (J. L.), MAXIMON (L. C.) and MORGAN (G. W.). — On the stationary "salt wedge" — a two layer free surface flow. *Graduate Division of Applied Mathematics*, Brown University, U.S.A., Technical Report No. 1 (1953).

[11] SCHIJF (J. B.) and SCHONFELD (J. C.). — Theoretical considerations of the motion of salt and fresh water. Proc. Minnesota International Hydraulics Convention, *5th Congress I.A.H.R.* (1953).

[12] HINWOOD (J. B.). — Estuarine salt wedges, determining their shape and size. *The Dock and Harbour Authority*, Vol. 65, No. 525 (July 1964), 79-83.

[13] MAJEWSKI (W.). — The outfall of waste waters, including the effect of density differences. Laboratory investigation on the arrested wedge. Proc. XIth Congress, *International Association for Hydraulics Research*, Leningrad (1965).

[14] FRAZER (W.), BARR (D. I. H.) and SMITH (A. A.). — Reply to discussion on a hydraulic model study of heat dissipation at Longannet Power Station. *Proc. Instit. of Civil Engs.*, Vol. 39 (January 1968), 23-44.

[15] WU (J.). — Laboratory results of salt water intrusion. Journal of Hydraulics Div., *Amer. Soc. of Civil Engs.*, 95, No. HY 6 (November 1969), 2209-2213.

[16] KEULEGAN (G. H.). — The Mechanism of an Arrested Saline Wedge. Chapter II, Coastal and Estuarine Hydrodynamics.

[17] SHARPE (J. J.). — Spread of buoyant jets at the free surface. *Journal of Hydraulics Div. Amer. Soc. of Civil Engs.*, 95, No. HY 3 (May 1969), 811-825).

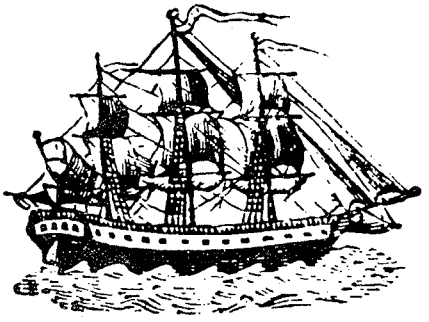

Voir résumé français à la page suivante

J. F. RIDDELL

Résumé

Les courants de densité en canal rectangulaire
IV. — Le coin salé en régime permanent

Le présent article est le quatrième d'une série comprenant quatre études sur les courants de densité dans les canaux de section rectangulaire. Il a trait à des recherches sur un type particulier de courant de densité, le coin salé en régime permanent. Une nouvelle forme de corrélation portant sur la similitude permet de regrouper les variables intervenant dans ce phénomène, et des équations sont établies, qui permettent de définir l'étendue de la pénétration saline.

A la place de l'élargissement classique du canal ayant pour objet de constituer « une mer », les auteurs ont implanté des « boîtes d'introductions » dans le canal, ce qui leur a permis d'exécuter des essais à grande échelle avec un canal de grande largeur.

En prenant en premier lieu comme variable résultante la longueur relative du coin salé mesurée de l'extrémité aval de celui-ci jusqu'à la hauteur relative du coin arbitrairement choisie, ils montrent que cette longueur relative augmente lorsque le nombre de Froude densimétrique décroît, ou que le nombre d'Archimède croît. Par contre, ils constatent que toute variation de la hauteur globale de l'écoulement modifie la longueur relative du coin salé, et ils montrent que, bien que le nombre de Froude densimétrique, le nombre d'Archimède et la largeur relative du canal restent égaux, la longueur relative augmente en fonction de la hauteur globale de l'écoulement.

La plus grande partie de l'interface d'un coin salé en régime permanent correspond à peu de choses près à une droite, dont les auteurs prennent la pente comme deuxième variable résultante. Ensuite, ils prouvent que cette pente représente une variable effective en ce qui concerne toutes variations des variables imposées, y compris pour des essais effectués avec des canaux de largeur relative allant jusqu'à 10.

Enfin les auteurs présentent un diagramme de congruence qui permet de calculer les pentes relatives du coin salé dans la nature, et ils donnent quelques indications sur les valeurs de la hauteur relative du coin salé correspondant en principe au début et à la fin de l'interface linéaire.